

Tunable coupling in synthetic oscillators for pattern recognition

Subramanian Sundaram

Introduction: Synthetic oscillators based on transcriptional regulators have received a lot of attention over last decade^{1, 2}. The motivations for this have been twofold: a) to understand the building blocks of time keeping, such as the circadian rhythm, pervasive in natural organisms, and b) as control blocks in applications such as bacterial lysis for *in vivo* drug delivery³. Over time, the precision in oscillation time scales and synchronization across large cell populations have been improved both spatially and temporally^{4, 5}. This was achieved by improving the speed of coupling using a shared post-translational coupling based on ClpXP protease degradation. While synchronized oscillators have been demonstrated, quorum of cells have not been used to perform coherent computations. In parallel, in the broad field of computing, interest in arrays of coupled oscillators with tunable coupling has grown based on their superior performance in pattern recognition and associative memory applications⁶. Theoretical proposals for such oscillatory systems exist⁷, but practical demonstrations have not been possible with challenges in large scale oscillator coupling.

The main objective of the project is to explore pattern recognition abilities of synchronized quorum of cells and understand convergence behavior of the oscillator networks. The oscillator network is simulated by developing a framework for solving delay-differential equations in MATLAB in time domain, as a 2D interconnected array of spatially coupled oscillators. Two different oscillator network topologies are compared and it is shown that a 4 element array demonstrates abilities to memorize patterns, even in the presence of noise. The convergence behavior depends on the hamming distance between the input and the memorized pattern.

Methods: The system described here consists of an array of synthetic oscillator cell colonies (P_i) each isolated in a physically defined well. The individual cells (*E. coli*) within a group P_i are fully coherent. Figure 1a shows an array of 4 cell populations. Each group is coupled with common cell population (shown in blue). Based on the nature of spatial coupling of each cell with the common population, the phase relationship between each well can be controlled.

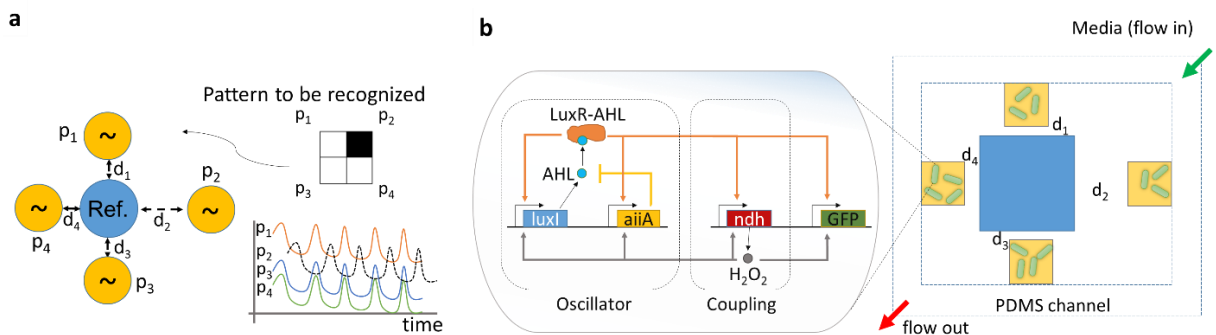


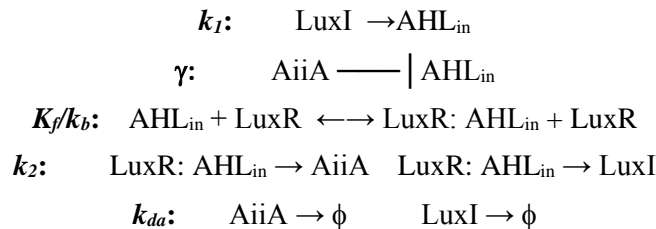
Figure 1. a. Overview of the coupled oscillators, a sample pattern to be recognized and the corresponding steady state oscillations of the cell groups where the relative phase denotes the information in the pattern to be recognized. **b.** The regulatory network inside each cell (based on reference 8) and the general physical configuration of cell colonies.

When all the cells are coupled uniformly, the oscillations are synchronized. When the coupling distance is increased, out-of-phase coupling can be achieved. The relative phase between the oscillators corresponds to the data in each individual pixel of the pattern to be recognized as shown in the right. Here, the white pixels are all in-phase (0°) but the black pixel is out-of-phase (180°) with the other pixels. The oscillations on the bottom show the converged states. The pattern to be matched is input as the initial phase to the respective cell group, where the time it takes to converge to the steady state is expected to give the hamming distance between the input pattern and the pattern to be recognized.

The array of cell groups (P_i) are built using a setup similar to the work of Prindle et al.⁸ where two hierarchies of coupling exist: short range but strong coupling (with AHL) and a longer range but weak coupling (with H_2O_2). The oscillation transcriptional network is shown in Figure 1b. It is assumed that LuxR is constitutively expressed here and that the expression of AHL is directly driven by the LuxI concentration. The LuxR-AHL hybrid controls the expression of LuxI, *aiiA*, *ndh* and GFP from four identical modules. Each of the cell colonies (P_i) consists of these cells with the oscillation-coupling network shown in the diagram. The colonies are isolated into PDMS wells with varying distance between them. The inter colony distance controls the in-phase/out-of-phase synchronization between the colonies with respect to the larger common reference population. There is no AHL diffusion between the individual cell colonies through the PDMS membranes since inter colony communication is primarily via gas phase. In this system, NDH-2 is a respiratory enzyme that is bound to the membrane that produces H_2O_2 . H_2O_2 permeates through the PDMS layer and inactivates the ArcAB which normally represses the expression of LuxI.

Initialization of phase in an array of oscillators is one of the key challenges in all practical demonstrations of synchronized oscillators. Here we overcome that by using high intensity blue light for this purpose. When high intensity blue light is turned on, the GFP acts as a photosensitizer and releases free radicals that produce reactive oxygen species including H_2O_2 . When the concentration of H_2O_2 is high the fluorescence remains in the high state and the oscillations are stopped. Using a digital logic projector (DLP), blue light can be individually turned on or off at each of the colonies, presenting a potential for easy large scale initialization of patterns. The time taken by the oscillator network after initialization to converge to the steady state phase differences, is set by the configuration of the PDMS well (and the well spacing).

The model is governed by the following kinetics^{5, 8}:



Transport processes:

Dilution of AHL_{out} by flow, $k_d: \quad \text{AHL}_{out} \rightarrow \phi$

Fick's diffusion of AHL_{out} , D_2

Convection of AHL between interior and exterior, D_1 : $AHL_{out} \longleftrightarrow AHL_{in}$

Oscillator governing equations:

$$\frac{\partial AHL_{in}}{\partial t} = \frac{c_1 LuxI}{k_1 + LuxI} - c_2 \frac{AiiA AHL_{in}}{\gamma + AHL_{in}} + D_1(AHL_{out} - AHL_{in}) \quad (1)$$

$$\frac{\partial AHL_{out}}{\partial t} = -k_d AHL_{out} - \frac{d}{1-d} D(AHL_{out} - AHL_{in}) + D_2 \frac{\partial^2 AHL_{out}}{\partial x^2} \quad (2)$$

$$\frac{\partial AiiA}{\partial t} = \alpha_1 \frac{AHL_{in}^2}{k_2 + AHL_{in}^2} - k_{da} AiiA \quad (3)$$

$$\frac{\partial LuxI}{\partial t} = \alpha_2 \frac{AHL_{in}^2}{k_2 + AHL_{in}^2} - k_{dl} LuxI \quad (4)$$

The above equations govern the bulk oscillator performance under the following assumptions:

1. LuxR is expressed constitutively and the concentration of LuxR is significantly high such that the kinetics of $AHL_{in}:LuxR$ formations are rapid and solely depend on AHL_{in} concentration.
2. The degradation of AHL_{in} can be ignored since the convection of AHL from the exterior and the repression of AHL by AiiA are bound to be dominant.
3. The local synchronization within a cell colony is not affected by H_2O_2 coupling
4. The direct coupling between H_2O_2 from two adjacent colonies is ignored and the primary mode of coupling is assumed to be between each colony and the common reference pool. This is reasonable since the distance between two colonies is typically significantly larger than the distance between a colony and the reference cell pool.

The parameters for oscillations in an individual colony can be optimized easily with the system of ODEs described above, but including spatial diffusion terms is computationally expensive.

To model the spatio-temporal interactions which are critical to model the oscillatory network, delay-differential equations are used as replacements; these have been found to effectively capture the oscillator dynamics in prior reports^{9, 8}. In order to account for the coupling between different spatial colonies, a simplified model⁸ is made accounting for colony averaged LuxI concentrations (X_i), based on delayed auto repression of LuxI and delayed activation by H_2O_2 concentration (H_i)

$$\frac{\partial X_i}{\partial t} = \alpha \frac{1 + \vartheta H_i \tau_2}{\left(1 + \frac{X_i \tau_1}{C_0}\right)^2} - \frac{\gamma X_i}{k + X_i} \quad (5)$$

Where the subscripts τ_1 , and τ_2 show delayed responses, for e.g., $H_{i,\tau_2}(t) = H_i(t - \tau_2)$. The main parameters here are α and γ which model the effectiveness of the delayed activation by H_2O_2 and the degradation of LuxI. C_0 and k allow control of the delayed auto repression by LuxI and the size of the cell colony. The H_2O_2 concentration in each colony can be described by

$$\frac{\partial H_i}{\partial t} = \mu + \alpha_h X_i - \gamma_h H_i + \hat{F}\{H_i\} \quad (6)$$

$F\{H_i\}$ denotes the effective flux of H_2O_2 diffusing in and out of each colony from the central reference cell population and the external sinks, and is described by the discretized version of the diffusion equation (j are all the neighboring entities)

$$\hat{F}\{H_i\} = \sum_j D \frac{(H_i - H_j)}{d_{ij}^2} \quad (7)$$

where D is the diffusion coefficient for the diffusion of H_2O_2 through the membrane.

Results:

Note that to solve the new system of equations (5)-(7), considering the diffusion terms in time and space, the *Parts and Compositors framework* cannot be used. A new MATLAB framework is developed with delay-differential equations solvers to test the oscillators and the network topologies. The parameters used for the simulations are obtained from Prindle et al.⁸ and modified to obtain the desired behavior. Typically $\alpha = 8.25$, $\gamma = 5.75$, $\nu = 1$, $\tau_1 = 20$, $\tau_2 = 10$, $c_0 = 6$, $k = 10$, $\mu = 20$, $\alpha_h = 1$, $\gamma_h = 10$, $D = 7$, $d_i = 1$ is used. Noise is introduced in the system by adding up to ± 0.25 to α and γ of each oscillator randomly. This corresponds to activation and degradation noise.

To test the individual oscillators, the above system is setup initially as a 1D oscillator connected to 0 concentration sinks at distance d_i on each side as shown in the inset in figure 2a. The buildup of oscillations is shown in figure 2b. As the distance to the sink is increased from 1 to 1.5, the oscillation time period increases as does the amplitude, as expected. This is because as the distance (or wall thickness) increases, the amount of H_2O_2 diffusing out decreases. The Fourier transform of the oscillation signals is shown in figure 2a.

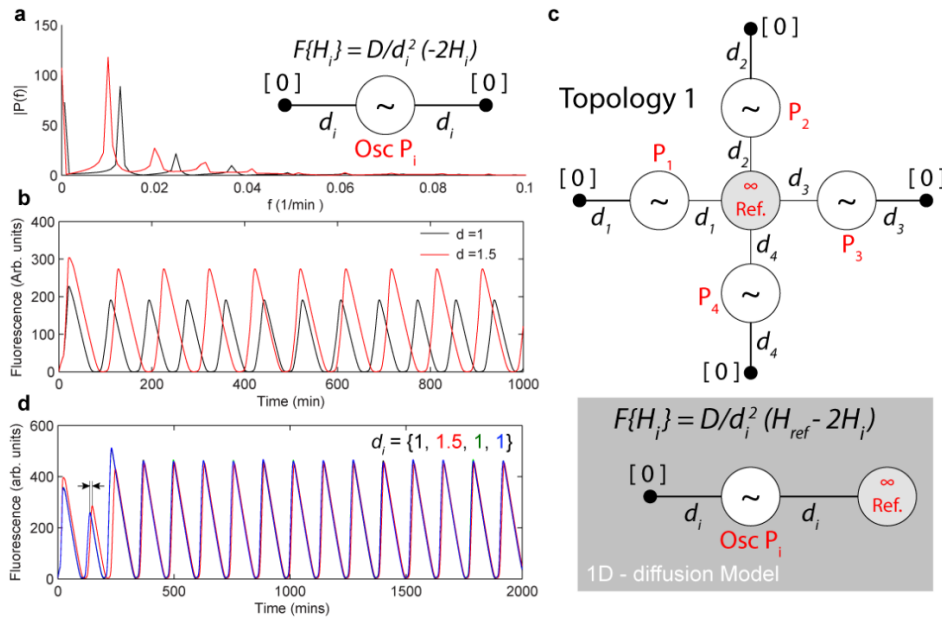


Figure 2. **a.** Fourier transform of the oscillation signals, and time evolution of the fluorescence in **b.** The inset in **a** shows the diffusion model for single oscillators. **c.** A 4 oscillator network connected to an infinite (or bulky) reference oscillator. The box in the bottom shows the 1D diffusion model used for each oscillator colony P_i . **d.** The oscillations in 4 colonies where one colony (P_2) is spaced far away ($d_2 = 1.5$) from the reference oscillator colony.

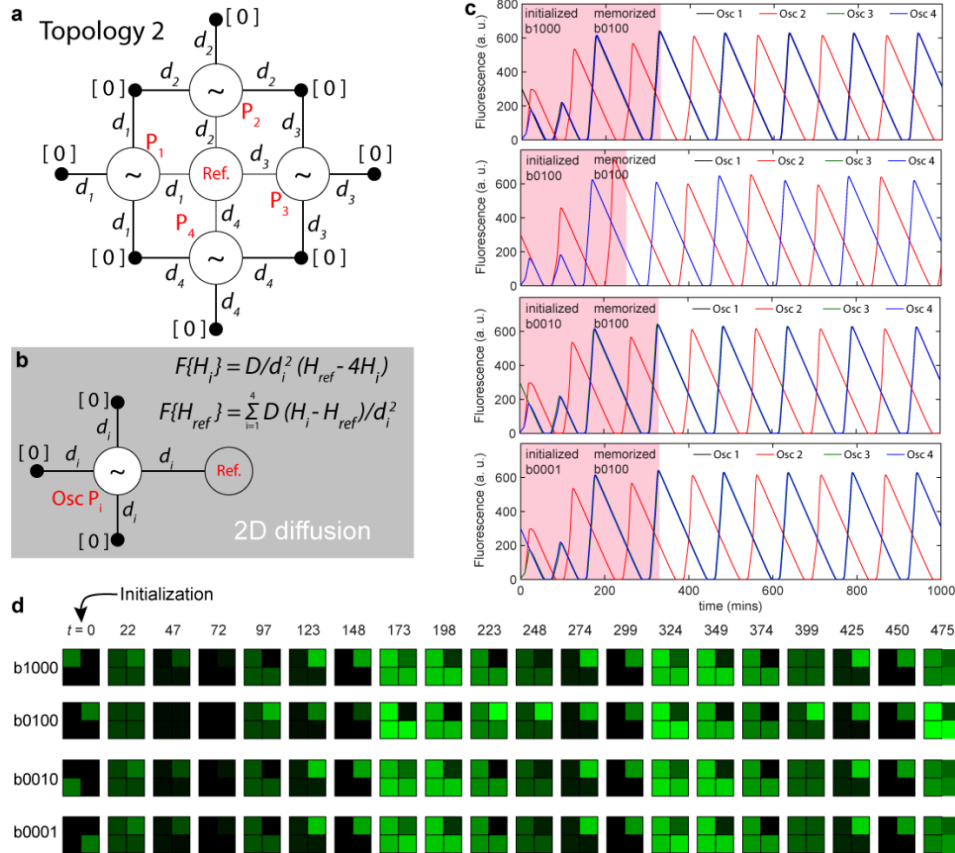


Figure 3. a. 4 oscillator array topology connected to a finite reference. The H_2O_2 concentrations from the neighbors P_i diffuse into the reference and affect the reference colony. **b.** The box shows the 2D discrete-diffusion model used in the simulations for each H_i and H_{ref} . **c.** The oscillations in a network with $d = \{0.75, 2, 0.75, 0.75\}$ stores the bit pattern ‘b0100’. When initialized with different inputs ‘b1000’, ‘b0100’, ‘b0010’ and ‘b0001’, the convergence times depend on the hamming distances to the memorized pattern, in this case, 2, 0, 2 and 2. **d.** The fluorescence in each pixel as a function of time (minutes) showing the 4 different initialization cases. In all cases the stable memorized pattern ‘b0100’ is reached.

To test of the possibility of making interconnected oscillator networks, 4 oscillators are coupled to a bulky or an infinite reference as shown in Figure 2c. Each of the 4 oscillator colonies can be modeled by a 1D diffusion system as shown in the box, as the bulky reference is large enough to be influence by the H_2O_2 diffusion from the individual oscillators P_i . When the system is setup with all distances d_i being the same except for d_2 , the phase starts to deviate initially but the bulky reference overpowers the P_2 into synchrony with the other oscillators as shown in Figure 2d. Improving the distance from the bulky reference did not lead to a stable phase offset as required.

The topology was modified into a network of oscillators shown in Figure 3a. In this case the reference oscillator is similar to all the individual colonies and stable phase offsets could be obtained even in the presence of noise. To memorize ‘b0100’ the distances were set to $d = \{0.75, 2, 0.75, 0.75\}$. Since the reference is influenced by the H_2O_2 diffusing from its neighbors, a 2D-diffusion model is required, as shown in Figure 3b. When the individual oscillators are initialized to ‘b1000’, ‘b0100’, ‘b0010’ and ‘b0001’, in all cases, the system converges to the memorized state, ‘b0100’ as shown in Figure 3c. The hamming distance for input ‘b0100’ is 0, while it is 2

for the other three cases. It is evident that the oscillations build up faster in the case of a 'b0100' initialization, demonstrating that convergence times depend on hamming distances even when the amount of H₂O₂ introduced in the system is equal in each case. Figure 4d shows the fluorescence intensities generated in these 4 runs with different initialization, as a function of time. At $t = 0$, the 2×2 array is initialized differently but reaches the same state by $t = 425$ min in all cases.

This work shows that coupled synthetic oscillators can be used in applications where independent oscillator colonies cooperatively work towards pattern recognition tasks even when noise is taken in to consideration. When patterns are initialized with blue light (leading to high H₂O₂ generation), the convergence behavior shows a relationship to the hamming distance between the input code and the memorized pattern. There are several directions to enhance this study. It is important to investigate larger arrays of oscillators, which at the same time also enables exploring more complex network topologies. Large scale quantitative studies of convergence behavior with several inputs of varying hamming distances, accounting for noise at multiple stages would be interesting to explore. These results may then provide a compelling case for experimental implementations of these interconnected oscillatory networks made of synthetic cell oscillators.

References:

1. Elowitz, M. & Leibler, S. A synthetic oscillatory network of transcriptional regulators. *Nature* **403**, 335-338 (2000).
2. Potvin-Trottier, L., Lord, N., Vinnicombe, G. & Paulsson, J. Synchronous long-term oscillations in a synthetic gene circuit. *Nature* **538**, 514-517 (2016).
3. Din, M. et al. Synchronized cycles of bacterial lysis for in vivo delivery. *Nature* **536**, 81-85 (2016).
4. Danino, T., Mondragón-Palomino, O., Tsimring, L. & Hasty, J. A synchronized quorum of genetic clocks. *Nature* **463**, 326-330 (2010).
5. Prindle, A. et al. Rapid and tunable post-translational coupling of genetic circuits. *Nature* **508**, 387-391 (2014).
6. Hoppensteadt, F. & Izhikevich, E. Oscillatory Neurocomputers with Dynamic Connectivity. *Physical Review Letters* **82**, 2983-2986 (1999).
7. Fang, Y., Yashin, V., Levitan, S. & Balazs, A. Pattern recognition with "materials that compute". *Science Advances* **2**, e1601114-e1601114 (2016).
8. Prindle, A. et al. A sensing array of radically coupled genetic 'biopixels'. *Nature* **481**, 39-44 (2011).
9. Mather, W., Bennett, M., Hasty, J. & Tsimring, L. Delay-Induced Degrade-and-Fire Oscillations in Small Genetic Circuits. *Physical Review Letters* **102**, (2009).